Adsorption Energy Distribution from the Aranovich−Donohue Lattice Density Functional Theory

P. Kowalczyk,* H. Tanaka, H. Kanoh, and K. Kaneko

Department of Chemistry, Faculty of Science, Chiba University, 1-33 Yayoi, Inage, Chiba 263-8522, Japan

Received September 18, 2003. In Final Form: December 25, 2003

We propose a new methodology projected for the estimation of the adsorption energy distribution from the monolayer part of a single nitrogen adsorption isotherm determined at 77 K based on the lattice density functional theory (DFT) via the Aranovich−Donohue formalism. At first sight, the presented approach is computationally more difficult than a classical one. However, it is more flexible and comprehensible. Next, we developed a numerical program and used it for the estimation of the adsorption energy distribution from the experimental data on carbon black samples. The main nitrogen molecule−carbon black surface interaction energy can be estimated as ≈7−8 kJ/mol, but the heterogeneity of the investigated materials differs significantly. Furthermore, we compare the results obtained from the lattice DFT via the Aranovich−Donohue formalism with the solution of the integral equation with the kernel represented by the classical monolayer localized Fowler−Guggenheim isotherm equation. The similarity between these two independent approaches is observed. The proposed methodology can be used for the investigation of the energetic heterogeneity of not only the carbonaceous materials but also the other "flat-surfaced" solids.

I. Introduction

It is generally believed that any adequate theory of adsorption on real surfaces must take into account the surface heterogeneity in adsorption energy (i.e., the molecule−surface dispersion interactions ϵ_s).[1−4] Of the numerous reasons for surface heterogeneity, we mention local variations in surface structure, variation in crystal structure, nonuniform distribution of surface groups, crystal defects, surface impurities, porosity, etc. The generally accepted quantitative measure of the energetic heterogeneity of surfaces is the differential distribution of the adsorption sites $f(\epsilon_s)$, among various values of the adsorption energy ϵ_s.[1−4] Mathematically, $f(\epsilon_s)$ can be determined by the inversion of the linear Fredholm integral equation of the first kind given by the following formula:[1−4]

$$\theta_g(p) = \int_a^b \theta(\epsilon_s,p)\, f(\epsilon_s)\, d\epsilon_s, \quad c \le p \le d \text{ (for } T = \text{const.)} \tag{1}$$

The kernel $\theta(\epsilon_s,p)$ represents the local adsorption model (i.e., local adsorption isotherm), $\theta_g(p)$ is the left-hand side of eq 1, frequently called the total adsorption isotherm (usually expressed by the fractional loading, surface coverage, adsorbed amount, etc.), which is experimentally measured, and $f(\epsilon_s)$ is the differential adsorption energy distribution (i.e., it is a relative number of adsorbing centers with the energy ϵ_s).

The physical meaning of $f(\epsilon_s)$ implies the properties of nonnegativity and normalization; thus,[5]

$$\forall\ \epsilon_s\colon f(\epsilon_s) \ge 0 \tag{2}$$

$$\int_a^b f(\epsilon_s)\, d\epsilon_s = 1$$

There are plenty of local adsorption models (i.e., isotherms) that can be substituted into eq 1 to represent the adsorption process on a homogeneous patch of surface.[1−5] Among them, the Langmuir, Frumkin [i.e., Fowler−Guggenheim (FG)], and Hill−deBoer models are the most frequently used.[1−5] All of the models that are mentioned above are characterized by some simplifications in the description of a gas-adsorption process.[1]

For example, the well-known localized Langmuir isotherm describes the monolayer adsorption with interactions only between molecules and the surface. The Langmuir isotherm can be written as follows:[6]

$$\theta(p,\epsilon_s) = \frac{K_1 p}{1 + K_1 p} \tag{3}$$

where p is the adsorbate gas pressure and the Langmuir constant K_1 is defined as[4,6]

$$K_1 = K_1^0(T)\, \exp(\epsilon_s/k_b T) \tag{4}$$

where k_b denotes the Boltzmann constant, T is the temperature, and $K_1^0(T)$ is the preexponential factor that contains the partition functions of an isolated molecule in gas and surface phases with rotational, vibrational, and translational degrees of freedom. It can be determined, for example, by Adamson's approximation.[4] As a result of neglect of the lateral attractive interactions in the surface

* Author to whom correspondence should be addressed. E-mail: pkow@pchem2.s.chiba-u.ac.jp. Fax: 81-43-290-2788. Phone: 81-43-290-2779.

(1) Rudziński, W.; Everett, D. H. *Adsorption of Gases on Heterogeneous Surfaces*; Academic Press: New York, 1992.

(2) Rudziński, W., Steele, W. A., Zgrablich, G., Eds. *Equilibria and Dynamics of Gas Adsorption on Heterogeneous Solid Surfaces*; Elsevier: Amsterdam, 1997.

(3) Do, D. D. *Adsorption Analysis: Equilibria and Kinetics*; Imperial College Press: London, 1998.

(4) Jaroniec, M.; Madey, R. *Physical Adsorption on Heterogeneous Solids*; Elsevier: Amsterdam, 1988.

(5) Cerofolini, C. F.; Re, N. *Riv. Nuovo Cimento Soc. Ital. Fis.* **1993**, *16*, 1.

(6) Jaroniec, M.; Brauer, P. *Surf. Sci. Rep.* **1986**, *65*, 65.

10.1021/la035748k CCC: $27.50
Published on Web 02/13/2004

phase, the Langmuir model cannot predict a phase transition at a surface.

The simplest extension of the localized Langmuir model known as the FG isotherm includes the nearest-neighbor interactions in the Bragg−Williams approximations.[1−5] The FG isotherm describing the localized monolayer adsorption on the "patch-wise" model of the surface topography can be written in the following form:[7]

$$\theta(p,\epsilon_s) = \frac{K_1 p \exp[c\omega\theta(p,\epsilon_s)]}{1 + K_1 p \exp[c\omega\theta(p,\epsilon_s)]} \tag{5}$$

where c is the site coordination number and ω is the nearest-neighbor interaction energy.[4] Besides that, this is the simple adsorption model capable of predicting a phase transition at a surface. This isotherm exhibits phase transition loops at temperatures lower than a critical temperature T_c, with $T_c = c\omega/4k^2$.

For the random model of the surface topography, the analogue of the FG adsorption isotherm is derived from the statistical thermodynamics by Hill, and it is given by[7]

$$\theta[p,\epsilon_s,\theta_g(p)] = \frac{K_1 p \exp[c\omega\theta_g(p)]}{1 + K_1 p \exp[c\omega\theta_g(p)]} \tag{6}$$

where $\theta_g(p)$ denotes the total adsorption isotherm. Clearly, the $c\omega\theta_g(p)$ term describes the average force field acting on an adsorbed molecule that arises from molecules located on the nearest-neighbor sites.

The Hill−deBoer mobile isotherm equation describes the adsorbate as a 2D van der Waals gas held at the surface by the adsorption field. In contrast to the localized models mentioned above, the Hill−deBoer mobile model assumes that molecules can diffuse freely on the surface. The Hill−deBoer isotherm equation can be written as[1−6]

$$p = p_v \frac{\theta(p,\epsilon_s)}{1 - \theta(p,\epsilon_s)} \exp\left[\frac{\theta(p,\epsilon_s)}{1 - \theta(p,\epsilon_s)} - \frac{a_2\theta(p,\epsilon_s)}{kT} - \frac{\epsilon_s}{kT}\right] \tag{7}$$

where p_v is the characteristic pressure and a_2 takes into account the interaction energy among the adsorbed molecules.

The qualitative behavior of this isotherm is roughly similar to that of the FG one. This equation exhibits the phase transition below a critical temperature T_c, with $T_c = 8a_2/27b_2k^2$.

Notice that all of the equations presented above consist of a physical constant, such as $K_1^0(T)$, $c\omega$, p_v, or a_2, that more or less influences the extent of the obtained results.

Recently, Aranovich and Donohue have proven that the classical models of the localized adsorption such as the Langmuir and FG isotherms are special cases of the statistical-lattice-gas approach, first introduced by Ono and Kondo.[8] Moreover, in a series of papers, Aranovich and co-workers generalized the Ono−Kondo statistical theory by employing the "thermodynamic" treatment.[9−18] The so-called Aranovich−Donohue formalism has the advantage of being much more flexible than the original derivation in that it allows one to model systems with complex boundaries (porous surface, multilayer adsorption on solid surface, etc.).[19] For these reasons, it is reasonable to use the Aranovich−Donohue approach for the investigation of the nature of both the molecule−surface and molecule−molecule interactions at low surface coverages (i.e., below monolayer completion). Clearly, the presented approach of the lattice density functional theory (DFT) is applicable only for the localized model of adsorption. However, the adsorption of gases (used as a standard method for the investigation of solid surfaces) such as nitrogen or argon at low temperatures can be suspected to be localized compared to a mobile one.[20,21]

The paper is organized as follows: In the first section, we present a brief description of the lattice DFT theory via the Aranovich−Donohue approach. Additionally, in this part of the paper, the concept of the adsorption energy distribution from the lattice DFT method is presented. In the second part, we briefly describe the regularization method used here for the inversion of the linear Fredholm integral equation of the first kind. Next, we present an illustrative example of the adsorption energy distributions evaluated from the lattice DFT based on the Temkin behavior. Moreover, the pure Temkin isotherm is used for the validation of the regularization algorithm proposed here. Finally, the low-temperature nitrogen experimental adsorption isotherms on carbon black samples are used for the validation of the developed method. The results are compared with the classical FG equation frequently used for the computation of the adsorption energy distribution function from the static adsorption data.

II. Lattice DFT

In this part of the paper, we consider the basic development of the lattice DFT via the Aranovich−Donohue formalism, and we present the concept of the adsorption energy distribution evaluated from the lattice DFT approach. Figure 1 illustrates the lattice model for both the multi- and monolayer adsorption.[22] The schematic representation of the molecule−molecule and molecule−surface interactions in the monolayer is also presented.

First, let us concentrate on the general description of the multilayer adsorption process on the homogeneous adsorbent surface. In the model presented in Figure 1, $i = 0$ represents the surface plane, $i = 1$ defines the first layer of adsorbate molecules, $i = 2$ defines the second layer, and so on. The last layer, $i = N + 1$, defines the bulk fluid.

According to the Aranovich−Donohue model, the multilayer adsorption process (see the upper part of Figure

(7) Heuchel, M.; Jaroniec, M.; Gilpin, R. K.; Brauer, P.; von Szombathely, M. *Langmuir* **1993**, *9*, 2537−2546.
(8) Ono, S.; Kondo, S. In *Molecular Theory of Surface Tension in Liquids, in Encyclopedia of Physics*; Flügge, S., Ed.; Springer: Berlin, Germany, 1960; Vol. 10, p 134.
(9) Aranovich, G. L.; Donohue, M. D. *J. Colloid Interface Sci.* **1998**, *205*, 121−130.
(10) Aranovich, G. L.; Donohue, M. D. *Phys. Rev. E: Stat. Phys., Plasmas, Fluids, Relat. Interdiscip. Top.* **1999**, *60*, 5552−5560.
(11) Aranovich, G. L.; Donohue, M. D. *J. Colloid Interface Sci.* **1999**, *213*, 457−464.
(12) Aranovich, G. L.; Donohue, M. D. *J. Colloid Interface Sci.* **2000**, *227*, 553−560.
(13) Aranovich, G. L.; Donohue, M. D. *Physica A* **1997**, *242*, 409.
(14) Aranovich, G. L.; Donohue, M. D. *Adv. Colloid Interface Sci.* **1998**, *76−77*, 137−152.
(15) Aranovich, G. L.; Donohue, M. D. *Comput. Chem.* **1998**, *22*, 429.
(16) Aranovich, G. L.; Donohue, M. D. *J. Colloid Interface Sci.* **1998**, *200*, 273−290.
(17) Sangwichien, C.; Aranovich, G. L.; Donohue, M. D. *Colloids Surf., A* **2002**, *206*, 313
(18) Hocker, T.; Aranovich, G. L.; Donohue, M. D. *J. Colloid Interface Sci.* **2001**, *238*, 167−176.
(19) Hocker, T.; Rajendran, A.; Mazzotti, M. *Langmuir* **2003**, *19*, 1254−1267.
(20) Olivier, J. P. *J. Porous Mater.* **1995**, *2*, 9.
(21) Ross, S.; Olivier, J. P. *On Physical Adsorption*; Interscience: New York, 1964.
(22) Aranovich, G. L.; Donohue, M. D. *Langmuir* **2003**, *19*, 3822−3829.

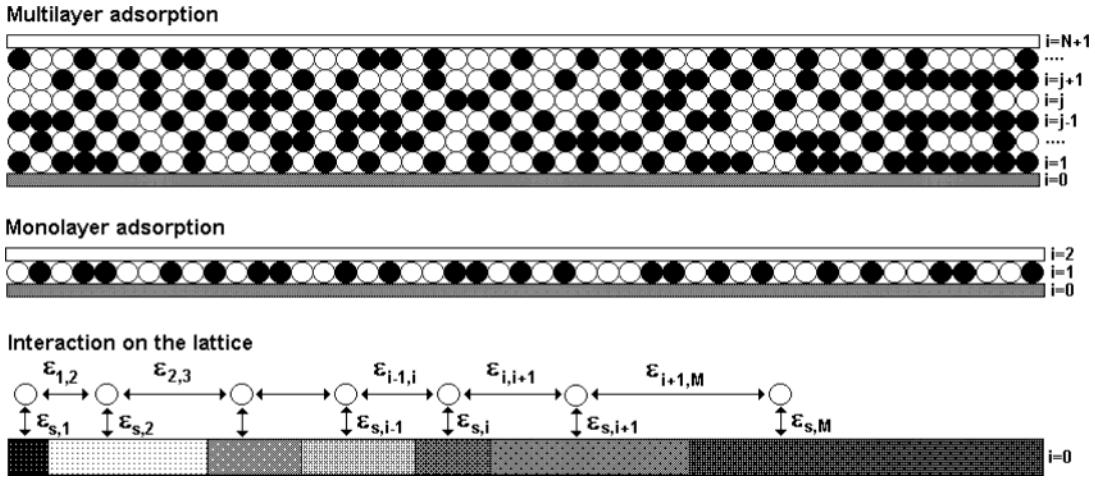

Figure 1. Schematic representation of the lattice model for multi- and monolayer adsorption. White circles represent the adsorbed molecules, and black ones, the vacancy. The interaction on the lattice includes both the molecule−surface and molecule−molecule interactions in the first layer (monolayer adsorption). Here, we assume that both $\epsilon_{1,2} \cong \epsilon_{2,3} \cong ... \cong \epsilon$ and $\epsilon_{s,1} \neq \epsilon_{s,2} \neq ... \neq \epsilon_{s,M}$ because of the surface disorder (heterogeneity).

1) on the cubic-type lattice can be described by the system of nonlinear finite-difference equations given by[14]

$$\ln\left[\frac{x_i(1-x_\infty)}{x_\infty(1-x_i)}\right] + \alpha(x_{i+1} + 4x_i - 6x_\infty) + \beta = 0 \quad \text{for } i = 1 \quad (8)$$

$$\ln\left[\frac{x_i(1-x_\infty)}{x_\infty(1-x_i)}\right] + \alpha(x_{i+1} + x_{i-1} + 4x_i - 6x_\infty) = 0 \quad \text{for } i = 2, 3, ..., N-1 \quad (9)$$

$$\ln\left[\frac{x_i(1-x_\infty)}{x_\infty(1-x_i)}\right] + \alpha(x_{i-1} + 4x_i - 5x_\infty) = 0 \quad \text{for } i = N \quad (10)$$

where

$$\alpha = \frac{\epsilon}{k_b T} \quad \text{and} \quad \beta = \frac{\epsilon_s}{k_b T} \quad (11)$$

Here, x_∞ denotes the bulk concentration, x_i is the concentration in the ith adsorbed layer, ϵ represents the nearest-neighbor energy of the adsorbate−adsorbate interactions, and ϵ_s is the interaction energy between the adsorbate molecules on the adsorbent surface. Both ϵ and ϵ_s are negative for the attractive forces.[22] Notice that the equations for $i = 1$ and $i = N$ define the boundary conditions on the lattice model.[14]

It is commonly known and generally accepted that the lower part of the adsorption isotherm (i.e., the part below the monolayer completion) is a source of information about the surface heterogeneity of the investigated material.[1−5]

On the basis of this assumption, eqs 8−10 can be simplified, leading to the Aranovich−Donohue monolayer adsorption isotherm describing the monolayer formation on the cubic lattice (i.e., $N = 1$, $x_2 = x_\infty$) given by[15]

$$\ln\left[\frac{x_1(1-x_\infty)}{x_\infty(1-x_1)}\right] + \alpha(4x_1 - 5x_\infty) + \beta = 0 \quad (12)$$

where x_1 denotes the concentration of the adsorbate in the monolayer.

The first derivative of eq 12 can be used for the construction of the so-called "path tracking algorithm" introduced by Aranovich and Donohue.[15] It is defined by

$$\frac{dx_1}{dx_\infty} = \frac{\dfrac{1}{x_\infty(1-x_\infty)} + 5\alpha}{\dfrac{1}{x_1(1-x_1)} + 4\alpha} \quad (13)$$

As mentioned earlier, Aranovich−Donohue derivations can generate typical monolayer adsorption isotherms like, for example, Henry's isotherm (i.e., the limit of low concentration)[17]

$$x_1 = x_\infty \exp(-\beta) \quad (14)$$

the Langmuir isotherm (i.e., hard-sphere behavior, for instance, no adsorbate−adsorbate interactions, $\alpha = 0$)[17]

$$x_1 = x_\infty/[x_\infty + (1 - x_\infty)\exp(\beta)] \quad (15)$$

and the Frumkin isotherm (i.e., $x_\infty \ll x_1$)[17]

$$x_1 = x_\infty[x_\infty + (1 - x_\infty)\exp(\beta + 4\alpha)] \quad (16)$$

The Gibbs excess adsorption can simply be obtained from the lattice DFT model and compared with the experimental data. Mathematically, the Gibbs excess is given by[17]

$$\theta \equiv \Gamma/\Gamma_m = x_1 - x_\infty \quad (17)$$

where Γ_m is the monolayer capacity.

It is very important to realize that eq 12, like equations presented in the Introduction, is valid for the hypothetical homogeneous surface. For the real surfaces (more or less heterogeneous), the molecule−surface atom interaction energy ϵ_s is supposed to be disordered (see Figure 1). So, in reality, the measured quantity such as Γ can be treated as a superposition of Γ's from each homostatic patch of a solid surface. Mathematically, according to the generally accepted integral theory of adsorption, eq 12 can be treated as a kernel of the following linear Fredholm integral equation of the first kind[1−5]

$$\theta(x_\infty) = \int_a^b [x_1(\beta) - x_\infty] f(\beta)\, d\beta, \quad c \le x_\infty \le d \text{ (for } T \text{ and } \alpha = \text{const.)} \quad (18)$$

Equation 18 can be solved numerically to get $f(\beta)$. Unfortunately, like other linear Fredholm integral equations, eq 18 belongs to the very difficult numerical problems known as the "ill-posed" ones.[1,2] Among the various numerical techniques projected for solving the "ill-posed" problems developed so far, regularization via Tikhonov's functional is treated as the most powerful.[23] For this reason, in the current paper, eq 18 is numerically computed by the well-known Tikhonov zero-order functional.[24] Because the solution of eq 18 is critical in the present approach, in the next part of this paper, we present a brief description of the regularization by the Tikhonov formalism.

III. Ill-Posed Problem

It is commonly known that the solution of the linear Fredholm integral equations of the first kind is not trivial.[23−25] For this reason, in this part, we pay attention to the main characteristics and methods of solution. The detailed characterization of the "ill-posed" theory is beyond the scope of this paper (the details can be found elsewhere[23−25]).

As we mentioned above, eq 18 is the classical example of an inverse ill-posed problem with a square-integrable kernel. It can be rewritten in a more general form[26]

$$\int_{\Omega(t)} K(s,t)\, x(t)\, \mathrm{d}t = y(s), \qquad s \in \Psi(s) \tag{19}$$

Square integrable means that the kernel $K(s,t)$ fulfills[23]

$$||K||^2 = \int_{\Omega(t)} \int_{\Psi(s)} |K(s,t)|^2\, \mathrm{d}s\, \mathrm{d}t < \infty \tag{20}$$

In a functional analysis setting, eq 19 is written in the operator form[27]

$$Kx = y \tag{21}$$

where K, called the kernel, is a compact Hilbert−Schmidt operator. In practice, K is given exactly by the underlying mathematical model. The function y, frequently called the right-hand-side, typically contains the measured quantities; i.e., y is only known with a certain accuracy and only in a finite set of points, $s_1, s_2, ..., s_M$. The inverse problem, i.e., finding x from K and y, is problematic because K is compact.[23] A compact K implies that the inverse K^{-1} is unbounded (if it exists!). The result is that the solution x cannot have a continuous dependence on y. This fact is mirrored in a linear system of the equations $Kx = y$ in the sense that the condition number is large. As a result, the solution x is extremely sensitive to an arbitrarily small perturbation in the right-hand-side y. In other words, the arbitrarily small amount of errors in y can lead to an arbitrarily large perturbation of the solution x.[28]

In physical terms, the integration with the kernel K in eq 19 has a "smoothing" effect on x in the sense that the high-frequency components, cups, and edges in x are "smoothed out" by the integration. We can therefore expect that the reverse process, i.e., computing x from y, will tend to amplify any high-frequency components in y. From the given properties, it is seen that the classical numerical methods of linear algebra, such as LU or Cholesky factorization, totally fail to compute a meaningful solution of x.[23−25]

The term "regularization" proposed by Tikhonov[29] and, independently, by Phillips,[30] is a common name for the methods to bound the unbounded K^{-1}. The regularized solution x_λ is the solution of the following minimization-smoothing functional (or Tikhonov's functional)[23−25]

$$x_\lambda = \min_x \left(||Kx - y||_2^2 + \lambda ||Lx||_2^2\right) \tag{22}$$

where λ is a positive number, usually called the Lagrange multiplier or regularization parameter, which controls the degree of regularization. The operator L introduces the "static penalty" if x behaves undesirably. The simple choice is to let L be the identity matrix, and hereby the regularization restricts the norm of x. Such a variant of the regularization method is commonly known as the smoothing functional with the zero-order stabilizing term.[31]

We can rewrite the linear operator equation of the first kind given by eq 21 in the form[32]

$$Kx = y, \quad K \in L(X,Y), \quad y \in Y, \quad x \in X \tag{23}$$

where X and Y are the real separable Hilbert's spaces and $L(X,Y)$ is the bounded linear operator mapping X into Y. Equation 23 can be called an exact equation. Now we introduce a family of equations[23,32]

$$K_\eta x = y_\delta, \quad K_\eta \in L(X,Y), \quad y_\delta \in Y, \quad x \in X \tag{24}$$

called the approximate equations, such that the inexact data (K_η, y_δ) approximate the exact data (K, y) with some known error of inexact data $\gamma \equiv (\eta, \delta)$ satisfying the following conditions:[23,24,32]

$$||K_\eta - K||_2^2 \le \eta, \quad ||y_\delta - y||_2^2 \le \delta, \quad ||K_\eta||_2^2 > \eta, \quad ||y_\delta||_2^2 > \delta \tag{25}$$

For a pair of inexact data (K_η, y_δ), there exists the unique regularization solution of eq 24 given by the Euler equation[32]

$$(K_\eta^* K_\eta + \lambda I) x_\lambda = K_\eta^* y_\delta \tag{26}$$

for Tikhonov's functional, i.e.,[32−34]

$$x_\lambda = (K_\eta^* K_\eta + \lambda I)^{-1} K_\eta^* y_\delta \tag{27}$$

where the asterisk denotes the transpose operation, I denotes the identity operator in a space Y, and $\lambda > 0$.

The matrix $K_\eta^* K_\eta$ in eq 27 is symmetric and positively defined.[23] Moreover, its eigenvalues are nonnegative.[23] If we add a positive constant λ to its diagonal, its eigenvalues will be greater than or equal to λ. If we select a suitable λ, the system of eq 27 becomes well-conditioned.

(23) Hansen, P. H. *Rank-Deficient and Discrete Ill-Posed Problems*; SIAM: Philadelphia, PA, 1992.
(24) Tikhonov, A. N.; Arsenin, V. Ya. *The Methods of Solution of Incorrect Problems*; Nauka: Moscow, 1979 (in Russian).
(25) Merz, P. J. *J. Comput. Phys.* **1980**, *38*, 64.
(26) Morozov, V. A. *Methods for Solving Incorrectly Posed Problems*; Springer: Berlin, 1984.
(27) Tikhonov, A. N.; Arsenin, V. Y. *Solutions of Ill-Posed Problem*; Winston & Sons: New York, 1997.
(28) von Szombathely, M.; Brauer, P.; Jaroniec, M. *Comput. Chem.* **1992**, *13*, 17.
(29) Tikhonov, A. N. *Dokl. Akad. Nauk SSSR* **1943**, *39*, 195.
(30) Phillips, D. L. *J. Assoc. Comput. Mach.* **1962**, *9*, 8.
(31) House, W. A. *J. Colloid Interface Sci.* **1978**, *67*, 166.
(32) Kojdecki, M. *Biul. Wojsk. Akad. Tech. im. Jaroslawa Dabrowskiego* **2000**, *49*, 1.
(33) Press, W. H.; Teukolsky, S. A.; Vetterling, W. T.; Flannery, B. P. *Numerical Recipes in Fortran*; Cambridge University Press: Cambridge, U.K., 1992.
(34) Koopal, L. K.; Vos, K. *Langmuir* **1993**, *9*, 2593.

The ways of selecting λ are very important in real computations. The bigger the λ is, the more stable eq 27 becomes and the farther the regularized solution is from the real solution. However, if λ is chosen to be small, eq 27 would not be well-conditioned.[23] In real computations, the best agreement between the theoretical model and experimental data is observed for $\lambda \rightarrow 0$.[28] However, the estimated x_η is dominated by a large negative (nonphysical) and positive oscillations.[28] An increase in λ smoothes x_λ, but simultaneously the agreement between the experimental and theoretical curves becomes worse.

From the above-mentioned considerations, it can be seen that the proper choice of λ is the real art of regularization algorithms. In most cases, the regularization parameter λ is chosen through a series of trials by an interactive judgment of the solution (i.e., by eye control). Usually as a starting point, a high-regularization parameter is selected, e.g., $\lambda = 1$, which results in a strongly smoothed solution x_λ. Subsequently, λ is reduced in an iterative fashion until the experimental accuracy is reached.[7,28]

Notice that such a method of λ selection is characterized by some drawbacks. First of all, the following selection procedure is very subjective and strongly depends on the user. Additionally, only the assumed global error in the right-hand side, i.e., δ, is taken into consideration. It is commonly known that the operator K is characterized by some amount of error because of the discretization of the continuous integral into discrete K_η by a quadrature. It is easy to show that if the number of discretization points increases, the obtained linear system is more ill-conditioned because of the similarity between the K_η matrix elements. Obviously, this selection procedure can be applied only by a very good specialist from the area of interest. A typical user can probably choose a totally uncorrected solution x_λ from the regularization family.

Moreover, it is well-known that to construct the regularization algorithm with good properties, a researcher should use all of the available information about the solution of the problem.[35] When we know nothing about the solution, then we may find anything as an approximate solution. Therefore, it is valuable to incorporate all of the available knowledge about the predicted solution, such as nonnegativity, monotonicity, convexness, boundedness of the first derivatives, and so on.[7,28,35] On the other hand, for instance, the nonnegativity of the obtained solution can suggest the improper assumption about the kernel in eq 18. Therefore, this criterion can be very helpful in the real computations to recognize a possible inadequacy.[34]

In light of the actual knowledge about the regularization method, the incorporation of additional constraints is very controversial. From our computer experiments as well as the fundamental work of von Szombathely and coworkers,[28] it can be concluded that the incorporation of the additional constraints such as nonnegativity is not necessary. Moreover, in this paper, we show that when the kernel in eq 18 is properly defined, the regularization with and without the nonnegativity constraint leads to the same results.

Recently, Hansen has summarized all methods used for the proper selection of the regularization parameter.[23] Additionally, he has shown that the so-called "L-curve" criterion proposed by Lawson and Hanson seems to be very promising.[36] For this reason, in this paper the "L-curve" criterion is used for the proper selection of the regularization parameter in the analysis of both sets of data, i.e., generated and experimental ones.

(35) Mamleev, V. Sh.; Bekturov, E. A. *Langmuir* **1996**, *12*, 441.
(36) Lawson, C. L.; Hanson, R. H. *Solving Least Squares Problems*; Prentice Hall: New York, 1974.

IV. Illustrative Example: Temkin Behavior on the Lattice

In this part, eq 18 is solved assuming both the Langmuir-type adsorption integral kernel and uniform form of the adsorption energy distribution function $f(\beta)$. As was shown by Rudziński and Everett, those assumptions lead to the well-known classical adsorption empirical isotherm equation commonly referred to as Temkin.[1] In all developed equations, we assume $c \le x_\infty \le d$.

In the first step, let us combine eqs 15 and 17 to obtain the kernel of eq 18

$$x_1(\beta) - x_\infty = x_\infty\left(\frac{1}{x_\infty + (1 - x_\infty)\exp(\beta)} - 1\right) \quad (28)$$

Next, let us assume the uniform form of $f(\beta)$, remembering the normalization property

$$\Psi = 1/(b - a) \quad (29)$$

Substituting eqs 28 and 29 into eq 18 gives

$$\theta(x_\infty) = \Psi x_\infty \int_a^b \left(\frac{1}{x_\infty + (1 - x_\infty)\exp(\beta)} - 1\right) \mathrm{d}\beta \quad (30)$$

Equation 30 can be solved analytically, and as a result, we obtain

$$\theta(x_\infty) = x_\infty \Psi\left\{\frac{1}{x_\infty}\ln\left[\frac{x_\infty \exp(a) - x_\infty - \exp(a)}{x_\infty \exp(b) - x_\infty - \exp(b)}\right] + \left(\frac{1}{x_\infty} - 1\right)(b - a)\right\} \quad (31)$$

Equation 31 can be treated as the analogue of the Temkin isotherm and, like a prototype, can be applied for the investigation of strongly heterogeneous surfaces.[1] This is beyond the scope of the present paper. However, eq 31 can also be used for testing of the numerical algorithm presented above. In the current paper, as usual, we generate some numerical data based on eqs 29 and 31. Moreover, some amount of Gaussian error is added to $\theta(x_\infty)$.[37,38] Next, the regularization algorithm is used to recover the original distribution function given by eq 29. Here, we want to point out that the assumed form of the distribution function is not trivial (i.e., characterized by discontinuities).

As one can observe in Figure 2, the regularization via Tikhonov's zero-order functional can reproduce original data from the noisy ones reasonably well. Notice that, as reported by many authors,[23] the regularization algorithm has the main problem at the discontinuous points. It is clearly visible in the case of thin peaks (see panel d in Figure 2). Obviously, nature does not like discontinuous points, and as a result, it is suspected that in real cases the peaks on the adsorption energy distribution should be Gaussian shape. Besides, all of our imaginary examples show the power of the presented regularization algorithm.

V. Describing the Experimental Data on Carbon Black Samples

Experimental verification of the presented theory and algorithm seems to be very important. For example, it is

(37) Gauden, P. A.; Kowalczyk, P.; Terzyk, A. P. *Langmuir* **2003**, *19*, 4253−4268.
(38) Gauden, P. A.; Terzyk, A. P. *Theory of Adsorption in Micropores of Carbonaceous Materials*; WICHiR: Warsaw, 2002 (in Polish).

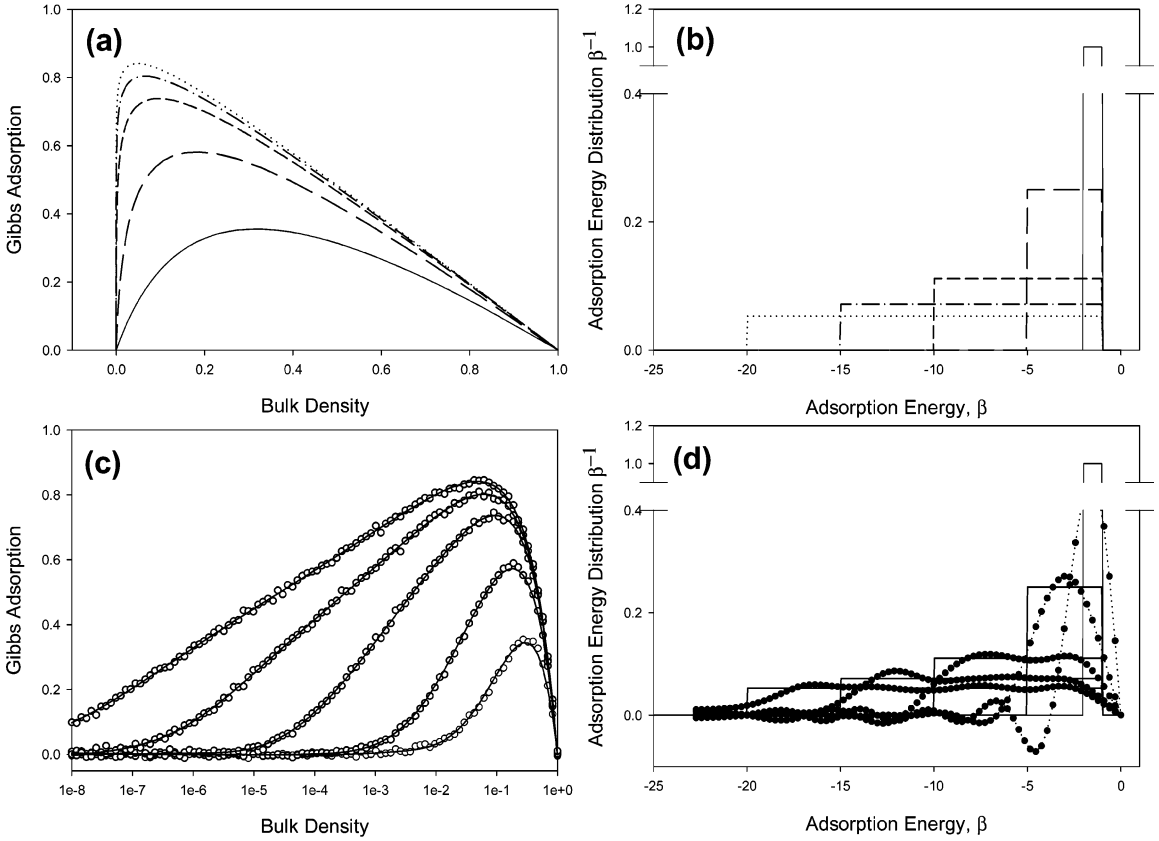

Figure 2. Illustration of the Temkin behavior on the lattice (see eq 31). Panel a represents the series of adsorption isotherms generated from eq 31 based on the assumed uniform adsorption energy distribution given in panel b. Panel c illustrates the recovery of the generated isotherms (solid lines) from the noisy data (open circles). Finally, panel d shows the assumed (solid lines) and recovered energy distribution functions by the Tikhonov zero-order functional.

Table 1. Sorption Characteristics of the Carbon Black Samples Studied

activated carbon black	a_m (mmol g^{-1})	S_{BET} (m^2 g^{-1})
Vulcan	0.84	82
SAO	0.98	96
M4040	0.83	81
M32B	0.75	74

very straightforward to show that for some cases the proposed theory or algorithm works very well with the generated data but totally fails for the real applications. Typical examples are given by Mamleev and Bekturov.[35] Among them, the application of the Fourier transform method by LamWan and White for the convolution-type integral equations seems to be very difficult in practice.[39] The mentioned Fourier smoothing-type analysis was tested for simulated distributions and showed good results. Unfortunately, the authors performed calculations for many points, $M = 1000$. In real cases, the number of experimental points obtained in the low-pressure region of the adsorption measurements is usually close to $M \approx 40$.[1−4] Additionally, the Fourier transform method can only be applied with the extension of the physical integration region $\Omega(\epsilon_s) \in (\epsilon_{s,min}, \epsilon_{s,max})$ to the unrealistic integration limits $(-\infty, \infty)$. This procedure can completely distort the obtained results, as was recently shown by Terzyk and co-workers.[40]

Four samples of carbon black were tested in this study. They are Vulcan, SAO, M4040, and M32B. All are commercial. The low-temperature nitrogen adsorption isotherms on Vulcan and SAO were taken from the literature.[41,42] The nitrogen adsorption isotherms at 77 K on Mitsubishi carbon black samples (M4040 and M32B) were carefully measured by the volumetric method.

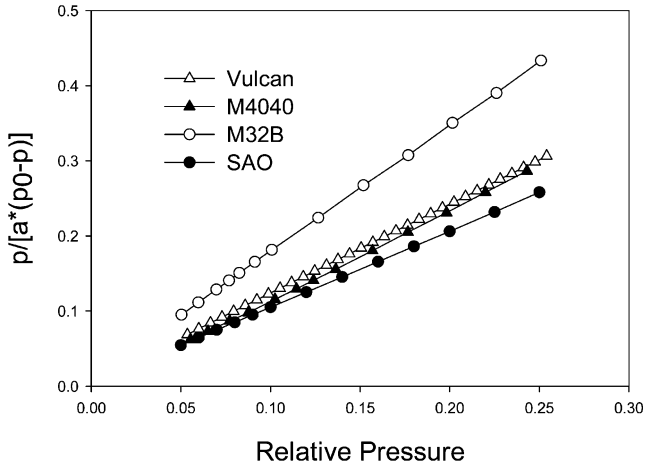

Figure 3. Experimental nitrogen adsorption data at 77 K plotted in the BET coordinates for carbon black samples.

First, the low-temperature nitrogen adsorption isotherms were used to evaluate such standard quantities as the Brunauer−Emmett−Teller (BET) specific surface area and monolayer capacity.[1−4] The total specific surface area was evaluated according to the well-known BET equation from the nitrogen adsorption data at the relative pressure range from 0.05 to 0.2. Table 1 summarizes the results. The comparison of the basic adsorption properties

(39) LamWan, J. A.; White, L. R. *J. Chem. Soc., Faraday Trans.* **1991**, *87*, 3051.
(40) Terzyk, A. P.; Gauden, P. A.; Rychlicki, G.; Wojsz, R. *Langmuir* **1999**, *15*, 285−288.

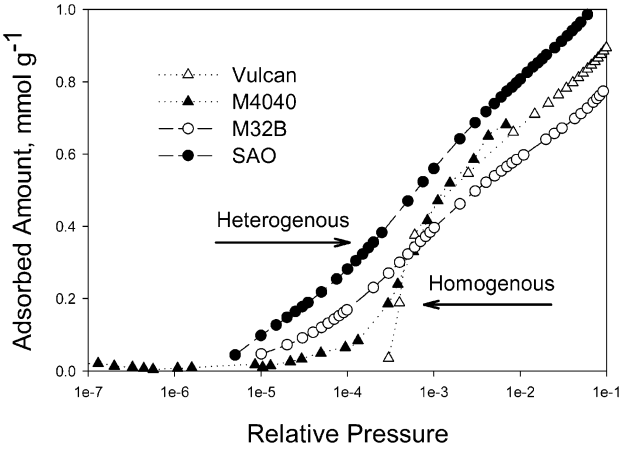

Figure 4. Low part of the experimental nitrogen adsorption isotherms at 77 K on carbon black samples.

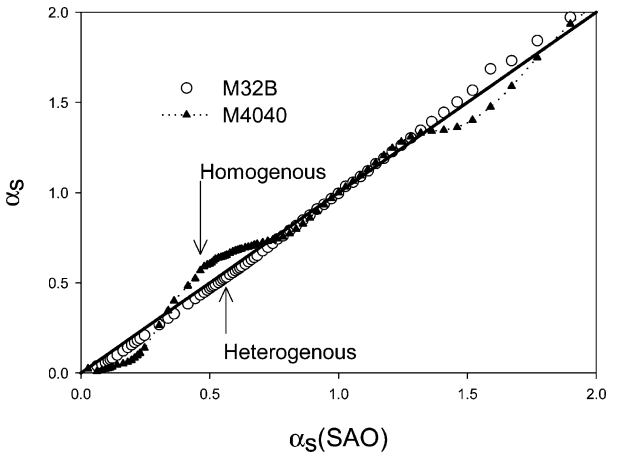

Figure 5. Comparative α_s plots of M32B and M4040 against the reduced standard adsorption α_s for SAO.

summarized in Table 1 and BET plots presented in Figure 3 indicates similar properties of the investigated materials. On the contrary, the low-pressure parts of the nitrogen adsorption isotherms displayed in Figure 4 clearly show the differences between the investigated materials. The classical adsorption books indicate that two of the studied carbon black samples (i.e., Vulcan and M4040) can be treated as homogeneous. The two remaining materials can be classified as heterogeneous. Notice that the heterogeneity is connected with the gradual shape of the monolayer adsorption isotherm.[43] The comparative plots of the reduced adsorption confirm this thesis. The strong oscillations characterizing the M4040B-activated carbon black suggest different energetic properties in comparison to SAO or M32B. On the other side, the similarity between SAO and M32B clearly shown in Figure 5 confirms the close energetic properties of both materials.

Obviously, detailed characteristics of the molecule−surface atom interactions can be obtained from the solution of the classical integral equations mentioned above or from the Aranovich−Donohue lattice DFT monolayer adsorption model. The first classical methods are well-described in different adsorption books.[1−4] The second one presented here is more difficult than inversion of the integral equation with Langmuir or FG kernel, but it is more

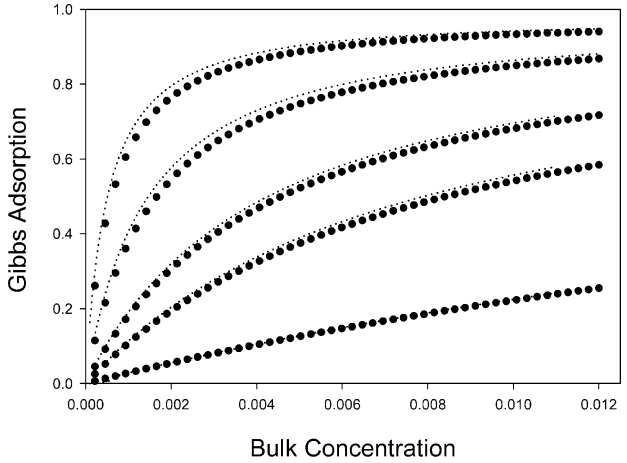

Figure 6. Gibbs monolayer adsorption isotherms generated from the Aranovich−Donohue lattice DFT for the Langmuir model (i.e., $\alpha = 0$) and the selected values of the molecule−surface interaction energy β: −7.4, −6.4, −5.4, −4.8, and −3.4. Dotted lines represent the computations performed by the "path-tracking algorithm", whereas the black circles are the results obtained by the "modified chord method".

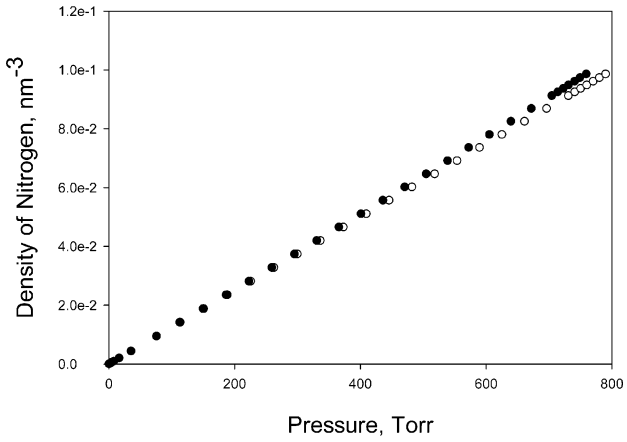

Figure 7. Relation between the density of nitrogen at 77 K and pressure computed by the equation of state (open circles) and simulation in the canonical ensemble via Widom's particle insertion technique (full circles).

flexible. Recently, Hocker and co-workers have presented a similar simplified approach, but only the theoretical data were considered.[18]

First, similar to Aranovich and Donohue, we point out that the kernel of eq 18 cannot be determined by the classical numerical algorithms.[15] In the current paper, we applied the "path tracking algorithm" proposed by Aranovich and Donohue as well as the "modified bisection (or chord) method" described by Kowalczyk and co-workers.[44] As an example, the comparison between these two algorithms is displayed in Figure 6. The agreement between these two alternative methods is observed. However, it is worth mentioning that the second method is more accurate and simple for application in practice.

Second, the relation between the dimensionless density on the lattice and measured relative pressure should be established. First, for this purpose, we adopted the simplest relation from the equation of state given by[9]

$$x_\infty = \frac{x_{\text{gas}}}{x_{\text{liquid}}} \tag{32}$$

where the density of the gas is defined by the equation of

(41) Fernandez-Colinas, J.; Denoyel, R.; Grillet, Y.; Rouquerol, F.; Rouquerol, J. *Langmuir* **1989**, *5*, 1205.
(42) Choma, J.; Jaroniec, M. *Pol. J. Chem.* **1997**, *71*, 380.
(43) Patrykiejew, A.; Sokolowski, S. *Adv. Colloid Interface Sci.* **1989**, *30*, 203.

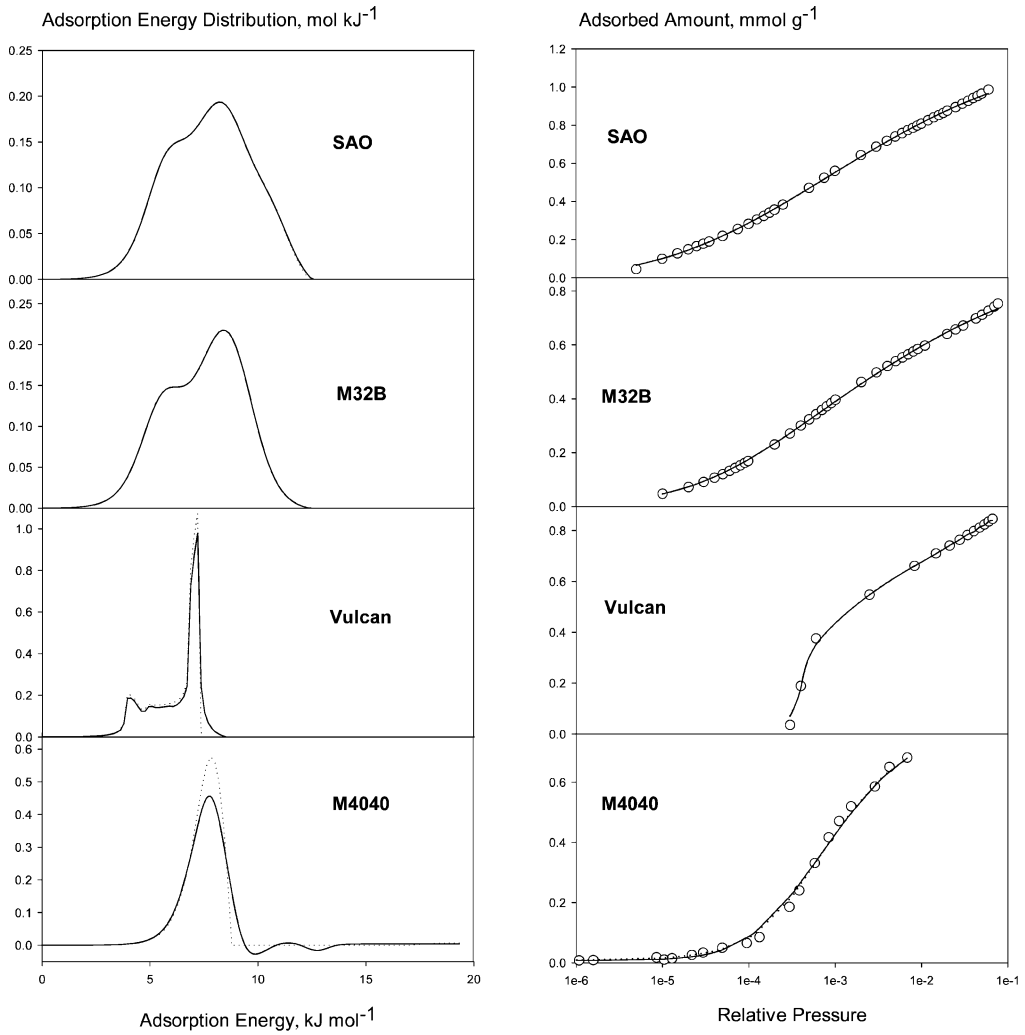

Figure 8. Adsorption energy distributions for carbon black samples obtained from the Aranovich−Donohue lattice DFT adsorption monolayer isotherm. Dotted and solid lines represent the solution of eq 18 obtained by regularization with the nonnegativity constraint and without this constraint, respectively. Open circles denote the low-pressure experimental data.

state $x_{gas} = p/RT$ and x_{liquid} is equal to 0.808 g/cm^3 for nitrogen at 77 K. Second, we used the simulation in the canonical ensemble by Widom's particle insertion method to correct the relation given by eq 32.[45,46] As one can see from Figure 7, at low pressures of nitrogen at 77 K, eq 32 is a very good approximation and can be used in real computations.

Third, notice that, in eq 18, we assume that the molecule−molecule interactions are known and constant (i.e., α = const.). This parameter was obtained from the fitting of eq 12 to the low part of the experimental nitrogen adsorption isotherms at 77 K. Moreover, it can simply be shown that if α is incorrectly estimated, it is impossible to obtain the stable solution from eq 18. This fact, i.e., difficulty, comes from the incorrect selection of the local adsorption model, is well-known, and is reported by several researchers.[25,31,34]

Knowing the relation between the quantities from the lattice model and experiment, as well as the mean molecule−molecule interaction energy α, we can invert eq 18 by the regularization method described above.

The final results obtained from the Aranovich−Donohue lattice DFT monolayer adsorption model are displayed in Figure 8. Notice that eq 18 describes the experimental low-pressure adsorption isotherm at 77 K reasonably well. Besides this, the evaluated adsorption energy distribution functions are characterized by the well-defined smoothed single peak. The broadening of the peak is strictly related to the heterogeneity effect. Thus, we can deduce that SAO and M34B carbon black samples are energetically heterogeneous. As a result, they should be used as the reference materials for the construction of the comparison plots in the case of activated carbons. For the materials, such as carbon nanotubes and nanohorns, i.e., characterized by a high homogeneity, the two remaining carbon black samples seem to be more reasonable.[47]

Finally, we present the comparison between the adsorption energy distribution functions obtained from the classical FG local monolayer adsorption isotherm and model presented above. The Langmuir constant for the adsorption of nitrogen at 77 K was taken for Puziy et al.,[48] while $c\omega$ was taken from Gun'ko et al.[49] As one can observe

(44) Kowalczyk, P.; Terzyk, A. P.; Gauden, P. A.; Solarz, L. *Comput. Chem.* **2002**, *26*, 125.
(45) Frenkel, D.; Smit, B. *Understanding Molecular Simulations: From Algorithm to Applications*; Academic Press: San Diego, CA, 1996.
(46) Patrykiejew, A. *An Introduction to Monte Carlo Method*; UMCS: Lublin, Poland, 1996 (in Polish).
(47) Kaneko, K.; Ishii, C.; Kanoh, H.; Hanazawa, Y.; Setoyama, N.; Suzuki, T. *Adv. Colloid Interface Sci.* **1998**, *76−77*, 295−320.
(48) Puziy, A. M.; Matynia, T.; Gawdzik, B.; Poddubnaya, O. I. *Langmuir* **1999**, *15*, 6016.
(49) Gun'ko, V. M.; Leboda, R.; Skubiszewska-Ziemba, J.; Turov, V. V.; Kowalczyk, P. *Langmuir* **2001**, *17*, 3148−3161.

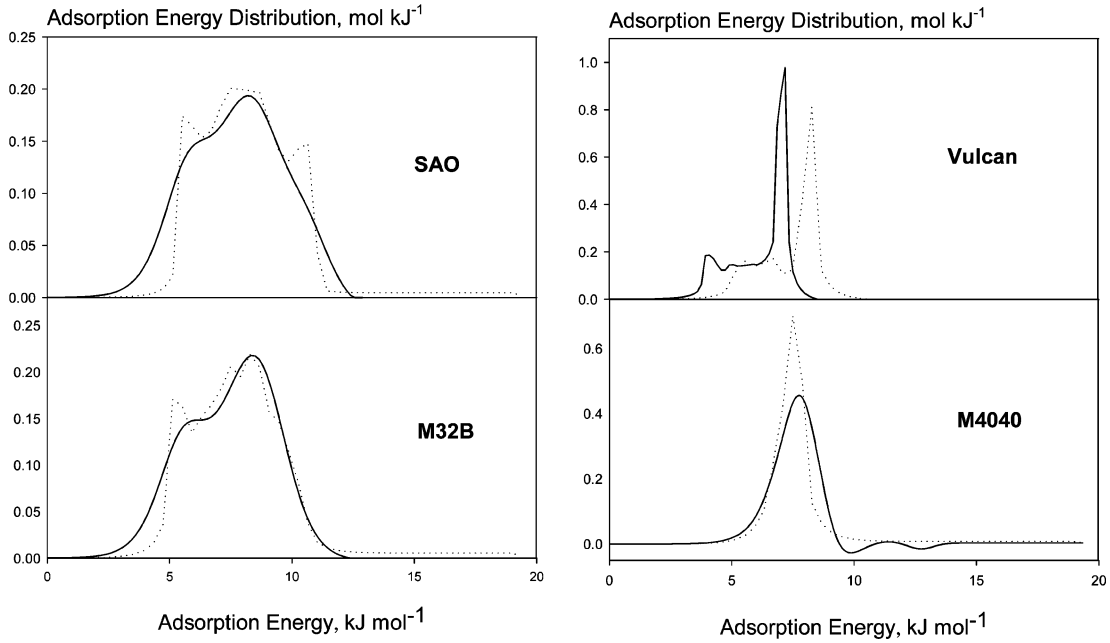

Figure 9. Adsorption energy distributions for the carbon black samples obtained from the Aranovich−Donohue lattice DFT adsorption monolayer isotherm (solid lines) and the classical localized FG monolayer model of adsorption (dotted lines).

in Figure 9, the agreement between these two independent methods is reasonably well, especially for strongly heterogeneous surfaces. The observed shift for the Vulcan-activated carbon black is attributed to the improper selection of the mean molecule−molecule interaction energy $c\omega$ or the Langmuir constant for the FG model. These parameters come from the quantum chemistry calculations and can be different than the real ones. Hence, the developed model based on the Aranovich−Donohue lattice DFT approach seems to be more flexible and comprehensible.

Acknowledgment. P.K. thanks Professor Aranovich for fruitful correspondences and Dr. A. P. Terzyk for critical suggestions and corrections of the manuscript.

LA035748K